ELSEVIER

Nuclear Physics A 640 (1998) 3–23

NUCLEAR PHYSICS A

Beta decay of ^{103}In: Evidence for the Gamow–Teller resonance near ^{100}Sn

M. Karny [a], L. Batist [b], B.A. Brown [c], D. Cano-Ott [d], R. Collatz [e], A. Gadea [d], R. Grzywacz [a], A. Guglielmetti [c,1], M. Hellström [e], Z. Hu [e], Z. Janas [a], R. Kirchner [e], F. Moroz [b], A. Piechaczek [f], A. Płochocki [a], E. Roeckl [e], B. Rubio [d], K. Rykaczewski [a,g], M. Shibata [e,2], J. Szerypo [a], J.L. Tain [d], V. Wittmann [b], A. Wöhr [f]

[a] *Institute of Experimental Physics, University of Warsaw, PL-00681 Warsaw, Poland*
[b] *St. Petersburg Nuclear Physics Institute, 188-350 Gatchina, Russia*
[c] *NSCL, Department of Physics and Astronomy, Michigan State University, East Lansing, MI 48824-1321, USA*
[d] *Instituto de Física Corpuscular, C.S.I.C.-University of Valencia, E-46100 Burjassot, Spain*
[e] *Gesellschaft für Schwerionenforschung mbH, D-64291 Darmstadt, Germany*
[f] *Instituut voor Kern- en Stralingsfysica, University of Leuven, B-3001 Leuven, Belgium*
[g] *Oak Ridge National Laboratory, Physics Division, P.O. Box 2008, Oak Ridge, TN 37831, USA*

Received 21 April 1998; revised 18 June 1998; accepted 7 July 1998

Abstract

The β decay of the neutron-deficient isotope ^{103}In was investigated by using total absorption γ-ray spectrometry on mass-separated sources. The measurement reveals a high-lying resonance of the β-decay strength in striking disagreement with high-resolution γ-ray data. The result is discussed in comparison with shell-model predictions. © 1998 Elsevier Science B.V.

PACS: 21.10.-k; 21.60.Cs; 23.40.Hc; 27.60.+j
Keywords: RADIOACTIVITY ^{103}In(β^+),(EC)[from ^{50}Cr(^{58}Ni, *xpyn*)]; measured E_γ, I_γ; deduced β-intensity and β-strength distribution. On-line mass separation, total absorption spectrometer, NaI(Tl) detectors, Ge-detector, Si-detectors.
NUCLEAR STRUCTURE ^{103}Cd, ^{103}In; calculated levels, Gamow–Teller strength.
SHELL MODEL

[1] Present address: Istituto di Fisica Generale Applicata dell'Universita di Milano, I-20133 Milan, Italy.
[2] Present address: Department of Energy, Engineering and Science, Nagoya University, Furo-cho, Chikusa-ky, Nagoya 464-01, Japan.

PII S0375-9474(98)00437-0

1. Introduction

Within the last few years, the region of nuclei near the doubly magic nucleus ^{100}Sn has been subject of intense experimental and theoretical investigations, see e.g. Refs. [1–4] and references therein. Although ^{100}Sn was observed by using high-energy fragmentation reactions, its detailed spectroscopy appears to be still out of experimental range. For nuclei *near* ^{100}Sn, however, both in-beam and decay spectroscopy is already feasible today.

One of the particularly interesting features of decay studies in the ^{100}Sn region is the occurrence of fast β transitions related to the Gamow–Teller (GT) transformation of a $\pi g_{9/2}$ proton into a $\nu g_{7/2}$ neutron. A measurable quantity suited for comparison with theoretical predictions is the β strength of this decay mode, defined as

$$B_{\mathrm{GT}}(E) = \frac{D \cdot I(E)}{f(Q_{\mathrm{EC}} - E) \cdot T_{1/2} \cdot 100}, \tag{1}$$

where $D = 3860(18)$ s is a constant, corresponding to the value of the axial vector weak interaction coupling constant g_A for the decay of the free neutron [5,6], I the β intensity normalized to 100% per decay, E the excitation energy in the daughter nucleus, f the statistical rate function, Q_{EC} the total energy released in electron-capture (EC) decay, and $T_{1/2}$ the β-decay half-life. The $B_{\mathrm{GT}}(E)$ distributions, deduced from measurements of $I(E)$, Q_{EC} and $T_{1/2}$, can be compared to the calculated square of the GT transition matrix element. The quenching of the experimental GT transition rates with reference to model predictions has been a puzzle for many years. A renormalization of g_A (or of the GT operator) has been applied (see e.g. Refs. [2,4]) in order to account for the missing GT strength in the ^{100}Sn region. This led to a consistent picture for the decays of even–even nuclei, with the GT strength from shell-model calculations being quenched by about a factor of 4 compared to experiment. However, the underlying β-decay data were limited so far. Furthermore, the dramatic reduction of the shell-model GT strength remained to be explained also for the decays of non-even–even nuclei (see Ref. [7] for a recent example).

On the basis of the extreme single-particle shell model, two main components are expected [4] in the GT decay of odd–even nuclei such as ^{103}In. There should be a single-particle transformation of an odd $\pi g_{9/2}$ proton into an excited $\nu g_{7/2}$ neutron state in the daughter nucleus ^{103}Cd. However, most of the GT strength should be carried by a transition corresponding to the decay of the even–even ($Z = 48$, $N = 54$) core of ^{103}In. This dominant transition, the "GT resonance", results from breaking of a pair of $g_{9/2}$ protons and forming the GT pair ($\pi g_{9/2}^{-1}, \nu g_{7/2}$) coupled to the odd $g_{9/2}$ proton in the daughter nucleus. Such three-quasiparticle states of three different final spins ($\Delta I = 0$ or ± 1 for GT decay) are located at relatively high excitation energies in the daughter nucleus, the residual interactions between the nucleons under consideration spreading the GT strength over many final states. This causes the intensity of individual β-delayed γ transitions in ^{103}Cd to be quite low, and their energies to be close to each other.

Classical high-resolution γ spectroscopy based on standard-size germanium detectors is generally unable, due to the relatively low efficiency of such detectors, to correctly record the intensity distribution of β-delayed γ rays emitted from nuclei far from the β-stability line. This is particularly true for high γ-ray energies (corresponding to high excitation energies in the daughter nucleus) and for low γ-ray intensities. Therefore, such experiments usually overestimate the β intensity for low-lying states, the resulting GT distribution being thus shifted towards low excitation energy. This effect causes an underestimation of the apparent total GT strength.

In order to improve the understanding of the origin of the GT quenching in general, and to avoid the inherent limitation of high-resolution γ spectroscopy, a program of investigating the β decays of non-even–even nuclei near ^{100}Sn by total absorption spectrometry has been initiated at the GSI on-line mass separator. This method, even with relatively low energy resolution, but with an efficiency as close to 100% as experimentally possible, is able in principle to resolve such complicated β-feeding patterns. Following a pilot study of ^{100}Ag [8], a six-quasiparticle configuration with respect to the ^{100}Sn core (three neutron particles and three proton holes), an improved total-absorption spectrometer (TAS) has recently been completed [9] and used for performing measurements on a series of neutron-deficient indium isotopes. In this paper, we report on a re-investigation of the β decay of ^{103}In, a five-quasiparticle configuration with respect to the ^{100}Sn core. The main goal of the experiment was to determine B_{GT} which, according to Eq. (1), can be deduced by measuring $I(E)$, Q_{EC}, and $T_{1/2}$. We performed a measurement of $I(E)$ by means of TAS, and took the values of Q_{EC} (6.05(2) MeV [10]) and $T_{1/2}$ (60(1) s [7]) from the literature. The experimental techniques applied in our experiment are described in Section 2. In order to estimate the systematic uncertainties involved in the evaluation of TAS data, we performed two independent evaluations. They differ in the applied Monte Carlo simulation codes, and in the assumptions made for the de-excitation pattern of high-lying ^{103}Cd levels. Details are presented in Section 3. In Section 4 we confront the experimental data with shell model predictions. Section 5 contains our summary.

2. Experimental techniques

2.1. General remarks on TAS

The TAS [9] consists of a large NaI crystal (diameter 356 mm, length 356 mm) surrounding the radioactive source, two small silicon (Si) detectors (thickness 450 μm, diameter 16 mm) above ("top") and below ("bottom") the source, and one germanium (Ge) detector (thickness 10mm, diameter 16 mm) placed close in the center of the NaI crystal just above the "top" detector. The NaI crystal is protected by a combined borax-lead shielding against room background including cosmic rays and accelerator-related background. By demanding coincidence with signals from the Si detectors, the β^+ decay component for the nucleus of interest is selected, whereas coincidences with characteristic $K_{\alpha,\beta}$ X-rays recorded by the Ge detector can be used to select the EC mode. In this way the *complete* distribution of the β strength can be determined for

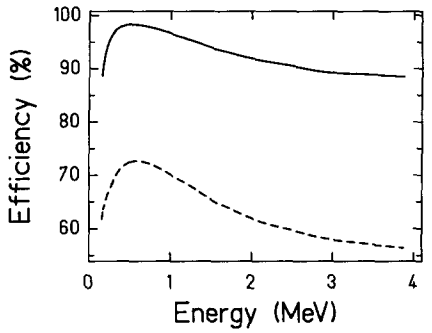

Fig. 1. TAS efficiency for monoenergetic γ rays, calculated by using the SIGMA code [11]. Displayed are the total efficiency (solid line) and the photopeak efficiency (broken line).

neutron-deficient isotopes, including low-lying *and* high-lying levels of the daughter nucleus. The coincidence option is particularly important, if the source strength is low and the signal-to-background ratio in singles spectra correspondingly small.

As can be seen from Fig. 1, the total γ-ray efficiency of TAS for monoenergetic photons between 0.2 and 4.0 MeV is above 88%, and its photopeak efficiency is above 56%. While the high efficiency values as well as their rather weak dependence on photon energy are promising, the problem of TAS measurements lies in the response function, the shape of which is complex already for single γ-ray sources. This is even more so for the case of large Q_{EC} values which lead to further complexity of $I(E)$ and of the related deexcitation in the daughter nucleus. Therefore, the determination of $I(E)$ from the experimental TAS spectra involves an intricate procedure. In the case of neutron-deficient isotopes, I represents the sum of EC and β^+ intensities, whereas the individual intensities are denoted by I_{EC} and I_{β^+}, and the intensity ratios I_{EC}/I and I_{EC}/I_{β^+} by EC/total and EC/β^+, respectively.

2.2. *Source preparation*

This work deals with the neutron-deficient isotope ^{103}In which was produced by means of ^{50}Cr(^{58}Ni,3p2n)^{103}In fusion-evaporation reactions. The energy and intensity of the ^{58}Ni beam on target amounted to 285 MeV and 40–50 particle nA, respectively. A 3.6 mg/cm^2 thick ^{50}Cr target, enriched to 96.2%, was used. The recoiling reaction products were stopped in a graphite catcher inside the gaseous discharge ion source of the GSI on-line separator [12] which provided a 55 keV mass-separated A=103 beam. The contaminations of ^{103}Sn and ^{103}Cd were strongly suppressed by choosing a FEBIAD-B2-C ion source with an alternately heated and cooled "cold pocket" which provides bunched indium beams [13], temporally separated from the tin or cadmium isobars. The ^{103}In beam, thus purified, was implanted into a transport tape. The resulting source was moved periodically every 100 s through a differential pumping system from the collection position (in vacuum) to the center of TAS (in air), where it was measured for 100 s. This timing, optimized for ^{103}In ($T_{1/2}$ = 60(1) s [7]), suppresses longer-lived

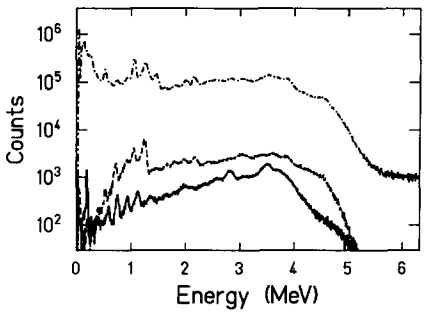

Fig. 2. TAS spectra obtained for the ^{103}In decay in singles (dash-dotted line) and in coincidence with β^+ and EC processes (broken and solid line, respectively).

activity such as the isobaric contaminant ^{103}Ag which is hardly attenuated in the ion source operation mentioned above. After three consecutive collection periods, the A=103 beam was directed for a 100 s interval to a separate tape collector which was equipped with a standard Ge detector for monitoring intensity and purity of the beam, while simultaneously a background measurement was performed at TAS. This mode of beam sharing between TAS and the monitoring station was continued for a total counting time of 22 hours. Fig. 2 shows the TAS spectrum obtained in this experiment for $A = 103$ sources, together with the EC and β^+ components used for the data analysis.

Although we used the bunched operation mode, the $A = 103$ beam used for the TAS measurements is not totally free of the isobaric contaminants ^{103}Cd and ^{103}Ag, especially since these also grow-in as decay daughters during the counting periods. Contributions from the decay of ^{103}Cd and ^{103}Ag as well as from room background are not harmful for the EC component of the ^{103}In decay, since the energy resolution of the Ge detector is sufficient to resolve X rays of palladium, silver, and cadmium. This is, however, not the case for the β^+ spectrum gated by signals from the silicon detectors. This condition suppresses the contribution from room background but not those from isobaric contaminants. In order to obtain a pure ^{103}In β^+ spectrum, we additionally measured the contributions from ^{103}Cd and ^{103}Ag in a separate experiment with 10 min collection and 180 min counting time. The resulting ^{103}Cd and ^{103}Ag β^+ spectra were then subtracted by using a normalization that was derived from the Ag and Pd X-ray intensities, respectively, measured by means of the Ge detector. Both the β^+ and EC spectra obtained in this way were corrected for pile-up effects. Details of this correction, which is based on a digitalized pulse shape, will be described elsewhere [14].

3. Data evaluation

3.1. General remarks on the unfolding procedures

In order to deduce the β-intensity $I(E)$ as a function of the excitation energy E in the daughter nucleus from an experimental TAS spectrum $S(x)$, one has to solve the

equation

$$S(x) = \sum_i R_i(x) \cdot I_i, \tag{2}$$

where I_i is the β-feeding to level i. Any column $R_i(x)$ of the response matrix, transformed from energy into experimental spectrum channels (x), represents the "level response function" of TAS to the cascade of γ rays deexciting the level i. $R_i(x)$ can be calculated recursively by using the response function for lower levels, as

$$R_i(x) = \sum_{k=0}^{i-1} b_{i\to k} \cdot \int R_k(x') \cdot G(E_i - E_k, x - x')dx', \tag{3}$$

where $G(E, x)$ is the TAS response function to the monoenergetic γ transition of the energy $E = E_i - E_k$, $b_{i\to k}$ the branching ratio for this transition, and $R_k(x)$ the level response function which is reduced to the δ function $\delta(x')$ in the case of a γ transition to the ground state $(k = 0)$. Since EC and β^+ spectra were extracted under different conditions (see Sections 3.2.2 and 3.3.2), the response functions used in data evaluation are supposed to be different.

In the case of TAS measurements of exotic nuclei one usually faces the problem that, even though some β-delayed γ rays are known from high-resolution measurements, many of them have escaped from observation in these experiments. Correspondingly, the decay schemes obtained from high-resolution data are incomplete, and hence assumptions have to be made in deducing I_i. Such assumptions may introduce *unpredictable* systematical uncertainties. Therefore, we decided to carry out two independent data analyses and to confront their results in order to estimate the systematical uncertainties.

The following two approaches were taken for choosing R_i and calculating I:

– First, we introduce, in addition to the ^{103}Cd states known from high-resolution work, "pseudo-levels" in ^{103}Cd with an intra-level spacing of approximately 50 keV. Furthermore, we assume R_i of a given pseudo-level to correspond to the average R_i of all unobserved levels. Such a procedure appears to be justified because of the poor energy resolution of NaI. The response function of a pseudo-level is constructed in the same way as for the known levels. Once the response functions are established for all levels, we sum them weighted with $I(E)$, and thus construct a simulated spectrum which is compared with the experimental one. In the following, this method is called recursive folding (RF).

– Second, we bin the experimental TAS spectrum into intervals of approximately 25 keV, assume a δ function for the shape of the photopeaks, and unfold the spectrum on the basis of "spectrum channels". The latter expression implies that every channel is treated as an independent region with respect to I and R_i. As a result of this simplification, Eq. (2) becomes a set of linear equations with a triangular matrix, which allows for an unambiguous decision by using the simple and fast "peel-off" (PO) procedure.

Insufficient assumptions on I and/or R_i result in deviations of the shape of simulated and experimental spectra, or in unphysical results emerging from the RF or PO methods,

respectively. The final solution is found by modifying the primary assumptions and checking the influence of such changes on the results.

3.2. Data evaluation based on the Recursive Folding Method

3.2.1. Response function determined by using the EGS code

The Electron-Gamma Shower (EGS) code was developed for a Monte Carlo simulation of the coupled transport of electrons and photons [15]. In our simulation, the EGS4 version of this code was used. For the purpose of the present work, TAS and its shielding was described as 54 coaxial regions (cylinders and annuluses). The center of the NaI crystal, i.e. the area around the radioactive sample, was divided into 28 regions. In order to speed up the calculation, regions which have no significant influence on the simulated spectrum were not taken into account. This condition is in particular fulfilled for the shielding materials (borax, lead). By using the simplified geometrical description based on coaxial regions like cylinders and annuluses, we neglected mechanical details such as the cold finger of the Ge detector, which is made of beryllium, as well as its aluminium housing. Furthermore, by approximating the TAS bore by a cylinder geometry, we neglected its actual key-hole shape. As a result of the approximation made in describing the TAS geometry, we had to modify the EGS calculation by including additional material in the center of TAS and by adjusting the density of the MgO material used as reflecting layer in the NaI crystal. These modifications were necessary for obtaining satisfactory agreement between simulated and experimental TAS spectra. The result obtained for the β decay of ^{24}Na is shown in Fig. 3.

To be able to evaluate the β^+ component of the spectrum, the knowledge of the response function for positrons is necessary. In view of the above-mentioned geometrical approximations we decided *not* to simulate a positron response function. Instead, we simulated the response function for the 511 keV annihilation quanta originating in the Ge detector. This procedure requires a special data treatment, to select only those events which fulfill the condition that positrons emitted from the center of TAS are stopped in the Ge detector.

To obtain the correct response function for a γ-ray cascade, a special calibration procedure, consisting of three steps, was used in the RF calculation. The first step took the production of light by *monoenergetic* γ rays into account, whereas in the second step *all* γ rays of the given cascade were included in a folding procedure to construct a "level response function" (see Eq. (3)). In a third step, the latter is recalibrated from "light equivalent units" to channels which can then be used to compare experimental and simulated spectra. Details of this procedure will be described elsewhere [14].

3.2.2. Treatment of EC and β^+ coincident data

When deducing I_{EC} and I_{β^+} as a function of E from TAS data, the influence of conversion electrons emitted in the deexcitation of ^{103}Cd levels has to be taken into account. The EC intensity was determined from the TAS spectrum, that was measured in coincidence with Cd X-rays recorded in the Ge detector and in anticoincidence with both

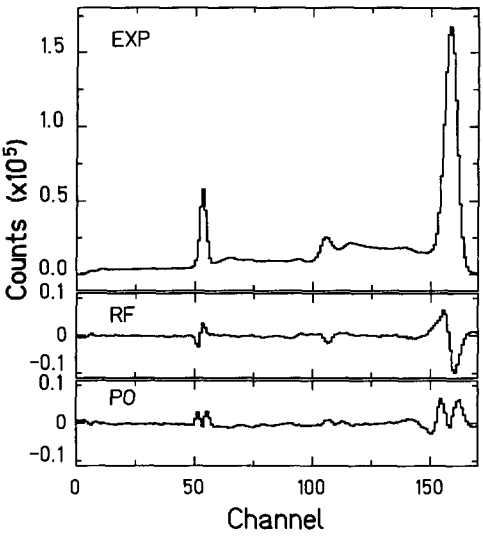

Fig. 3. TAS spectrum measured with a ^{24}Na source in comparison with results obtained by a simulation. The upper panel shows the experimental result, while the differences between experimental and simulated spectra, generated by using the recursive-folding (RF) method and the peel-off (PO) approximation, are displayed in the central and lower panel, respectively.

Si detectors. The latter requirement suppresses conversion-electron events occurring after EC and β^+ decays. The β^+ spectrum was obtained by demanding coincidence between signals from the NaI detector, the top Si detector, and the Ge detector operated at low gain. The Si-Ge coincidence represents a ΔE–E device which assures that a positron induced an energy-loss signal in the Si waver and was stopped in the Ge detector. Furthermore, it suppresses events associated with β^+-delayed conversion electrons.

3.2.3. Deconvolution procedure

The RF deconvolution procedure consists of 5 steps, which were repeated until a satisfactory result was obtained:

- the assumption concerning R_i for all pseudo-levels in the daughter nucleus ^{103}Cd;
- calculation of the response function for the pseudo-levels and levels;
- the assumption of a EC or β^+ population of those levels;
- calculation of the simulated spectrum,
- adjustment of the EC or β^+ population in order to minimize the differences between simulated and experimental spectrum.

As a first approach to construct a simulated spectrum, we used the decay scheme of ^{103}In deduced from high-resolution γ-ray data [7]. A comparison between the experimental EC spectrum from the present work and that simulated on the basis of the high-resolution data is presented in Fig. 4. Although the known decay scheme comprises over 50 levels and 100 γ-ray transitions [7], it is in striking disagreement with the new results obtained in this work.

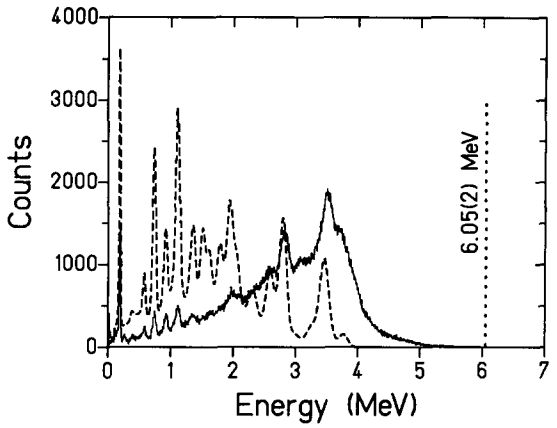

Fig. 4. Experimental TAS spectrum related to the EC component of the ^{103}In decay (solid curve), in comparison with the simulated spectrum (broken curve) obtained by the recursive-folding method with input data based on high-resolution work [7].

As a second approach in finding suitable values for the excitation energies of the pseudo-levels and the related R_i values, we started from ^{103}Cd levels that were identified by Szerypo et al. [7], and used γ rays which were observed by these authors but not placed in the decay scheme. Allowing variations of ± 2 keV we introduced more than 40 pseudo-levels, with an average of 3.5 deexciting γ rays per level and a spacing of approximately 50 keV between neighboring levels. In this approach, the γ rays from the high-resolution work, that were *not* placed in the decay scheme, served as a basis for constructing the pseudo-levels. Therefore, the total γ intensity obtained by the RF method exceeds that found by Szerypo et al. [7]. Furthermore, the mean γ-cascade multiplicity (m_γ), used for the simulation of the EC and β^+ spectra, was 3.2 and 2.5, respectively, i.e. considerably higher than the value of 2.0 suggested by the high-resolution data [7]. Fig. 5 shows the RF simulation, obtained for the EC component of the ^{103}In decay, in comparison with the corresponding experimental TAS spectrum.

In connection with this procedure, we had to normalize the experimental EC and β^+ spectra. This task was achieved by confronting the EC/β^+ ratio for a given energy level, resulting from the comparison of simulated and experimental EC or β^+ spectra, to the theoretical EC/β^+ ratio [16]. The energy interval can be chosen in two different ways. The first approach uses an interval, where both the EC and the β^+ spectrum have sufficient statistics, i.e. for ^{103}Cd excitation energies between 2.1 and 3.5 MeV. The second approach is based on the full energy range from 0 up to Q_{EC}, and uses the *divergence* of the normalization factor as information on experimental uncertainties including those from the data evaluation. The latter procedure is justified, since in the case of an ideal (uncertainty free) experiment and data evaluation, the ratio between theoretical and experimental EC/β^+ values should be constant without any divergence. The normalization factors calculated by both methods agree with each other within the respective uncertainties. However, the divergence of the values obtained from the second approach is higher. For the following data evaluation, the normalization coefficient

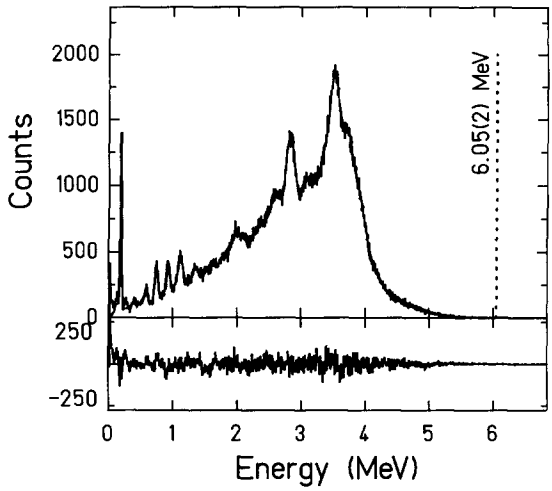

Fig. 5. Experimental TAS spectrum related to the EC component of the ^{103}In decay (upper panel) and difference between experimental data and results obtained by using the recursive-folding method (lower panel).

derived from the full energy interval was used.

After this normalization, the feeding to low-lying ^{103}Cd states is taken from the "reconstructed" β^+ spectrum, while the EC feeding is used for highly excited states. As this normalization depends on the Q_{EC} value, the uncertainty of the latter contributes to the uncertainty of the B_{GT} distribution. The resulting EC/total ratio is 0.46(4). Using this value we obtained a $\sum B_{GT}$ value 2.54(25), the uncertainty including contributions from counting statistics (0.15) and from the uncertainty of the EC/β^+ ratio (0.20).

3.3. Data evaluation based on the peel-off approximation method

3.3.1. Response function determined by using the SIGMA code

The SIGMA code [11] has been developed to simulate the response function for the total absorption spectrometer which has been used at the IRIS facility of PNPI in St. Petersburg, Russia. In this code, the geometry of the detector is described as a set of coaxial and enclosed cylinders. For the simulation of the response function of the TAS, the geometry was approximated by 15 cylinders. In addition, changes were introduced into the code in order to take into account the key-hole shape of the well of the main NaI detector. For fine tuning, the thickness of the aluminium wall of the well was varied in order to obtain best agreement between simulation and experimental data for the calibration sources. Fig. 3 shows a comparison between those spectra for ^{24}Na. In the simulation of the response functions, the non-proportionality of the NaI light output was taken into account by using the corresponding energy calibration for the photopeak position of monoenergetic γ rays. The remaining distortions due to this non-proportionality were relatively small owing to the folding procedure applied during the calculation of the level response functions for the cascades of γ rays (see Eq. (3)).

3.3.2. Treatment of EC and β^+ coincident data

In order to correct the experimental EC and β^+ spectra with respect to, e.g., the influence of conversion electrons, the PO approach was performed in an iterative way. In every step of the data evaluation, the response matrix was used to simulate the respective TAS spectra. Following a first assumption needed for the calculation of the response matrix, we arrived at preliminary deconvolutions. The resulting spectra were then used for simulating the corrections of the experimental spectra, and the whole deconvolution procedure was repeated (see Section 3.3.3). The response matrices obtained after the first iterations provided simulations with sufficient accuracy. This approximation seems justified, as the deconvolution-simulation cycle leads to a "damping" of uncertainties in the response matrices, and as the corrections under consideration were estimated to be relatively small.

The EC-decay data, selected by setting a coincidence condition on the Cd X-rays observed in the Ge detector, were corrected for contributions from conversion electrons. The latter were simulated and subtracted by using a normalization based on the intensity of the 1022 keV line observed in the Ge detector in coincidence with signals from the silicon detectors. The β^+ spectrum was obtained requiring coincidence between signals from the NaI detector and the top Si detector. The admixture of EC-decay events followed by electron conversion was calculated and subtracted. This calculation was based on the spectrum measured in the NaI detector in coincidence with the Ge and Si detectors, the threshold in the Si detectors being set high enough to reject conversion electrons. A contribution from EC-decay events was subtracted, which stemmed from registration of γ quanta in the top Si detector and was simulated to be about 3%.

3.3.3. Deconvolution procedure

Similar as in the RF method, the PO deconvolution of TAS spectra is based on results obtained by high-resolution γ spectroscopy. In accordance with the dominant structures of the experimental spectra, the 55 levels deduced in Ref. [7] were reduced into 17 "groups" of levels, a given group containing a single level or several close-lying ones. The experimental spectrum was binned into 25 keV intervals, and the response function was constructed for every bin. As the initial states are interrelated with the bins, the notation i of the initial levels in Eqs. (2) and (3) had to be replaced by a bin number. The values of γ branchings from the nth bin to the kth level, $b_{n\to k}$, were supposed to obey the dependence

$$b_{n\to k} = b_k \cdot (E_n - E_k)^3. \tag{4}$$

Within the framework of the PO method, the distributions of I_{EC} and I_{β^+} can be unambiguously calculated by using Eqs. (2), (3) and (4), provided the coefficients b_k are defined. Together with I, the total intensities of γ rays (I_γ) is then calculated for all 17 groups. One may safely assume that the high-resolution study [7] correctly determined the I_γ data for the low-lying ^{103}In levels. Thus, the PO iteration procedure was applied to find the 17 coefficients b_k from the condition that the I_γ values obtained

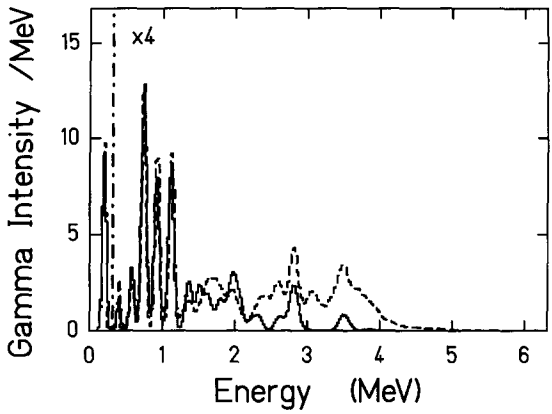

Fig. 6. Intensities of β-delayed γ-rays from the ^{103}In decay as a function of the ^{103}Cd excitation energy. The TAS data, deduced by using the peel-off method (broken line), are confronted to results from high-resolution work [7], which were folded with the TAS resolution (solid curve). Note the multiplication factor of 4, applied for ^{103}Cd excitation energies above 0.25 MeV.

from the PO method are equal to those given in [7]. This procedure was applied for both EC and β^+ spectra under the following two constraints:

- The calculated feedings to the regions between the well-resolved low-lying levels should be close to zero within the statistical uncertainties.
- The EC/β^+ values for low-lying levels should be in agreement with the ratio of the respective statistical rate functions [17].

The Q_{EC} value and normalization factors for the EC and β^+ spectra were determined in each iteration in the way described in Section 3.3.4.

Fig. 6 shows the I_γ data derived from [7] and from the present work. As can be seen from this figure, good agreement is obtained for the low-lying ^{103}In levels. However, a striking difference occurs a higher ^{103}In excitation energies. Most of the additional γ intensity, deduced from the TAS data, occurs in an excitation-energy range between 2.5 and 4.0 MeV. It is not surprising that such a distribution of I_γ over many levels remained unobserved in the high-resolution study.

The mean multiplicities of γ quanta for the EC and β^+ decay, derived from a deconvolution procedure of the I_{EC} and I_{β^+} distributions, amounts to 2.5 and 3.0, correspondingly. As can be deduced from the I_γ data displayed in Fig. 6, the mean multiplicity m_γ, following the EC/β^+ decay of ^{103}In, is 2.7.

3.3.4. Determination of the Q_{EC} value and β-strength distribution

The values of I_{EC} and I_{β^+} for the ^{103}In decay can be deduced, as an alternative to the determination of these quantities by the RF method (see Section 3.2.3), by decomposing the single TAS spectrum $S_{TAS}(x)$ into two components $S_{TAS}^{(EC)}(x)$ and $S_{TAS}^{(Si)}(x)$, respectively,

$$S_{TAS}(x) = c_{EC} \cdot S_{TAS}^{(EC)}(x) + c_{\beta^+} \cdot S_{TAS}^{(Si)}(x). \tag{5}$$

$S_{TAS}^{(EC)}$ and $S_{TAS}^{(Si)}$ were obtained from the corresponding coincidence spectra, taking the difference in the response functions for singles and coincidence spectra into account. The parameters c_{EC} and c_{β^+} were calculated by using the χ^2 method for $E \geqslant 3$ MeV. In this range of excitation energies, contributions from the isobaric contaminants (^{103}Cd, ^{103}Ag) are negligible.

Using this procedure, we calculated EC/total to be 0.44(2), in agreement with the value of 0.46(4) obtained by means of the RF method (see Section 3.2.3). The uncertainty of 0.02 was deduced from a χ^2 procedure, and includes a contribution from an estimate of the isobaric contamination.

In order to test the consistency of this procedure of EC/total determination, we used an alternative way to normalize the experimental EC and β^+ spectra. The latter approach, based on correlations between EC/β^+ and the ratio of the statistical rate functions for EC and β^+ decay f_{EC}/f_{β^+} [17], is similar to that used in Section 3.2.3. We considered Q_{EC} and EC/total as variable parameters to secure that EC/β^+ is equal to f_{EC}/f_{β^+} for any E within a sufficiently wide interval. From applying a χ^2 procedure within an E interval from 2.5 to 4.0 MeV, we obtained a Q_{EC} value of 6.02(10) MeV and a EC/total ratio of 0.46(4). These results agree with the Q_{EC} value of 6.05(2) MeV from the literature [10], and with the EC/total ratio determined from the decomposition of the singles spectrum, respectively.

As the uncertainties resulting from this two-parametric χ^2 procedure are rather large, it is preferable to perform a χ^2 fit for only one of the parameters, while fixing the other parameter. By using the EC/total value of 0.44(2), calculated above on the basis of Eq. (5), we obtained a Q_{EC} value of 6.04(6)MeV. The uncertainty of the latter result includes the uncertainties of the TAS energy calibration and of EC/total. This Q_{EC} value is in good agreement with the literature value of Q_{EC} = 6.05(2) MeV [10], which we prefer in the following due to its higher accuracy. Keeping this Q_{EC} value fixed in the one-parameter fit, we obtained EC/total = 0.45(2). Averaging this result with the value of 0.44(2) mentioned above, we deduced a recommended EC/total value of 0.445(20) for ^{103}In. We used this value for the normalization of I_{EC} and I_{β^+} in the PO method and for the corresponding determination of $I(E)$.

The B_{GT} distribution, calculated from these data according to Eq. (1), is displayed in Fig. 7. The resulting $\sum B_{GT}$ value is 2.40(25). Using the χ^2 analysis for the fixed value of Q_{EC}, we estimated the average uncertainty of I_{EC}/I_{β^+} to be 20%. This is valid for the 100 keV bins and the excitation energy interval of 2.5–4.0 MeV. By considering the uncertainties for I_{EC} and I_{β^+} to be independent, we obtained an uncertainty of about 15% for the I values of any of the 100 keV bins within an energy range between 2.5 and 4.0 MeV. This corresponds to an uncertainty of about 10% for $\sum B_{GT}$.

3.4. Uncertainties of the deconvolution of TAS spectra

Besides the *statistical* uncertainties, *systematical* uncertainties have to be taken into account in the deconvolution procedure, which may stem from incorrect assumptions concerning

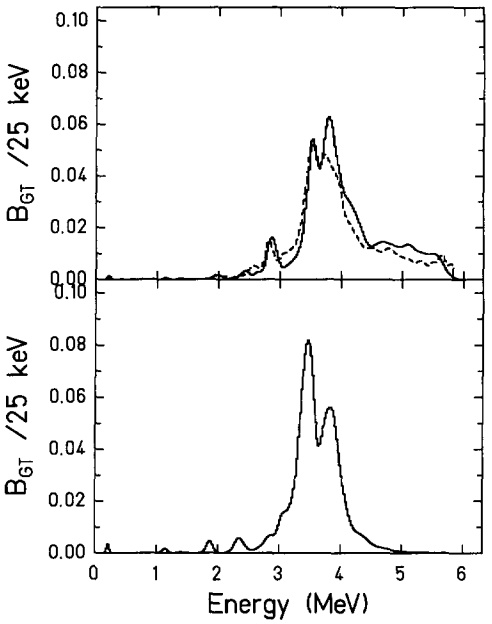

Fig. 7. B_{GT} values for the ^{103}In decay as a function of the ^{103}Cd excitation energy. Upper panel: TAS data derived by the recursive-folding (RF) method (solid line) and the peel-off (PO) approximation (broken line); lower panel: results obtained by the shell-model calculations using the small model space. For a direct comparison with the PO data, the B_{GT} values from the RF method and from the shell-model calculations were folded with the TAS resolution. Furthermore, the shell-model B_{GT} values were divided by a factor of 5.1.

- the level scheme of the daughter nucleus;
- the simulation of the response function, and
- the penetration of positrons into the NaI detector.

The uncertainty related to an incorrect assumption concerning the level scheme is difficult to evaluate analytically. By varying the γ branches within the limits of the imposed constraints, we estimated that the relative variation of $\sum B_{GT}$ does not exceed the difference between the values derived from the RF and PO approaches. It is clear, however, that the most important contribution is due to the uncertainty of the average multiplicity of γ quanta (δm_γ), which leads, via the level response function (R_i), to the uncertainties of the I value. As a rough approximation, we assume

$$\frac{\delta\epsilon}{\epsilon} = \delta m_\gamma |\ln(\epsilon_{max})|, \tag{6}$$

with ϵ being the TAS efficiency for full-energy absorption associated with a level of the excitation energy E, $\delta\epsilon$ the related uncertainty, and ϵ_{max} the maximum photopeak efficiency for monoenergetic photons. The latter was assumed to be ≈ 0.70 (see Fig. 1). As m_γ for high excitation energies is dominated by EC decay, we used the m_γ values of 3.2 and 3.0, suggested by the RF and PO evaluations, respectively (see Sections 3.2.3 and 3.3.3), to estimate δm_γ as 0.2. The corresponding $\delta\epsilon/\epsilon$ value amounts to about 7%, with the influence of ϵ_{max} uncertainties being neglected.

The spread of m_γ in the deexcitation of the levels populated by β decay give rise to "statistical" fluctuations in the experimental TAS spectra. During the deconvolution procedure, these fluctuations influence the calculated I values. The corresponding relative fluctuations of I, $\delta I/I$, can be approximated by

$$\frac{\delta I}{I} = |\ln(\epsilon_{\max})| \cdot \sqrt{3/2 \cdot D \cdot (m_\gamma - 1)/(\sqrt{\pi}\sigma)} \cdot \exp[-(\Delta E)^2/8\sigma^2]. \quad (7)$$

D is the mean spacing of (unobserved) levels, which is averaged with the TAS energy resolution (FWHM) by using a common response function (σ = FWHM/2.35), and ΔE is the energy interval of the fluctuations. The spread in B_{GT} for the levels is supposed to obey the Porter–Thomas law. A value of D = 3.3 keV for the allowed spins in the region of the B_{GT} maximum was derived from shell-model calculations. With the experimental FWHM value of 160 keV and the above-mentioned m_γ value of 3.2–3.0, we obtained a statistical B_{GT} uncertainty of approximately 8% for a ΔE value of 100–150 keV. Uncertainties related to the fluctuation of δm_γ contribute more to the *shape* of the B_{GT} distribution than to the $\sum B_{GT}$ value.

The value of δm_γ also influences the accuracy of the energy calibration. Due to the non-proportionality of light collection in the NaI crystal, a given channel of the experimental TAS spectrum can not be unambiguously related to a single E value, as this channel contains contributions from different γ-ray (or level) energies. Correspondingly, the uncertainty δE of the energy calibration due to this non-proportionality can be estimated as $\delta E = 31$ keVδm. A deviation in the I distributions obtained by the RF and PO approaches can also arise from the different assumptions made for the respective calibration procedures (see Sections 3.2.1 and 3.3.1).

In order to clarify a possible distortion of the experimental spectra due to positrons penetrating into the NaI detector, a separate measurement was performed with a polyethylen absorber below the bottom Si detector. Due to this absorber, positrons emitted from the source had to pass a polyethylen layer that was at least 20 mm thick. For energies above 0.5 MeV, no significant difference was found in the spectra gated by the top and bottom Si detectors. Thus we conclude that the results, obtained for I_{β^+} by gating on the top Si detector, are free from positron penetration effects in good approximation.

Additional uncertainties arise from the use of the Q_{EC} value of ^{103}In, especially in the case of the RF method. However, due to the high accuracy of the experimental Q_{EC} value (6.05(2) MeV [10]), this source of uncertainties has been neglected.

In comparison with the *systematical* uncertainties that were described above, those due to limited statistics are of importance only for excitation energies above 5.2 MeV. Being about 10% for a 100 keV bin at this energy, the uncertainty increases with E. Therefore, the region of reliable data is limited to the range $E \leqslant 5.5$ MeV. Nevertheless, the behavior of B_{GT} below this limit does not show any evidence of significant B_{GT} changes occuring around Q_{EC}.

In summary, the resulting B_{GT} uncertainties are somewhat smaller than those calculated on the basis of the divergence of the EC/β^+ renormalization factor (see Sec-

tions 3.2.3 and 3.3.4). This is due to the uncertainties associated with the simulation of the response function for monoenergetic γ rays as well as with the simplification made for the analytical estimate of the uncertainty presented above.

4. Results and discussion

4.1. Compilation of experimental results

The B_{GT} distributions for ^{103}In, obtained from the RF and PO methods (see Fig. 7), agree in the *gross* features, i.e. the dominant resonance around $E = 3.8$ MeV with a full width at half maximum of the order of 0.7 MeV. A closer inspection shows, however, that the B_{GT} resonance is split into two components, and that a long tail extends towards high excitation energies. Furthermore, distinct differences occur between the results obtained by the two unfolding procedures, concerning, e.g., the high-energy peak of the resonance. These differences, which are interpreted as representing the systematical uncertainties involved in these procedures, concern more the shape than the summed B_{GT} values $\sum B_{GT}^{(exp)}$ of 2.54(25) and 2.40(25) obtained from the RF and PO methods, respectively. The $\sum B_{GT}^{(exp)}$ value of ^{103}In recommended from this work is 2.47(25) as an average of the two results.

The mean multiplicities of γ cascades for the EC and β^+ component, obtained from the RF method, amount to 3.2 and 2.5, whereas the corresponding values, deduced from the PO method, are 3.0 and 2.5, respectively. The EC/total ratios determined by both methods agree within the respective uncertainties, yielding a recommended value of 0.445(20) (see Sections 3.2.3 and 3.3.4).

4.2. Shell model calculations

The model space and interaction we have used for the analysis of the ^{103}In GT β-decay is that denoted by SNB in [2], where it was introduced to calculate β-decay properties for nuclei near ^{100}Sn, in particular, for those with $N = 50$. The active orbits for protons are $p_{1/2}$ and $g_{9/2}$, and the active orbits for neutrons are $g_{7/2}$, $d_{5/2}$, $d_{3/2}$, $s_{1/2}$ and $h_{11/2}$. The SNB Hamiltonian is described in [2]. The β^+/EC GT strength within in the SNB model space arises only from the transition between a proton (π) in the $g_{9/2}$ orbital to a neutron (ν) in the $g_{7/2}$ orbital. The strength for this transition is maximized in the closed-shell $(\pi g_{9/2})^{10}$ 0^+ configuration for ^{100}Sn, with $B^o_{GT} = 17.78$ for the transition to $(\pi g_{9/2})^9;\nu g_{7/2}$ 1^+. In the general case, if the g_j orbit occupancies are N_j in the initial state, the total β^+/EC GT strength summed over all final states is $\sum B_{GT} = (N_{9/2}/10)(1 - N_{7/2}/8)B^o_{GT}$.

For ^{103}In it is possible to calculate the wave function for the initial $9/2^+$, $T = 5/2$ state in the full SNB configuration space $(\pi p_{1/2},g_{9/2})^{11};(\nu g_{7/2},d_{5/2},d_{3/2}, s_{1/2},h_{11/2})^4$. For this state $N_{9/2} = 9.0$ and $N_{7/2} = 1.66$ giving $\sum B_{GT} = 12.7$. An important question for the present experiment is how much of this strength lies at ^{103}Cd excitation energies which

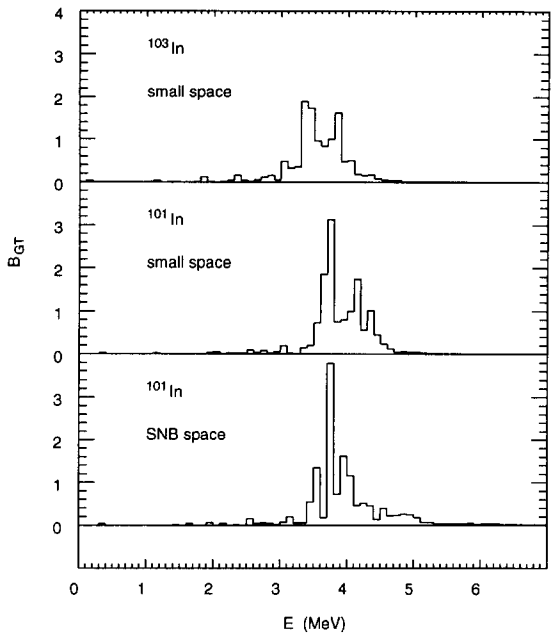

Fig. 8. B_{GT} distributions obtained from shell-model calculations by using the small model space for ^{103}In (upper panel) and ^{101}In (central panel), and by using the SNB model space for ^{101}In (lower panel).

are within the ^{103}In Q_{EC} window and the TAS detection sensitivity. The dimensions for the final state configuration $(\pi p_{1/2},g_{9/2})^{10}$; $(\nu g_{7/2},d_{5/2},d_{3/2}, s_{1/2},h_{11/2})^5$ are much too large to handle in a practical calculation (on the order of 100 000 states). However, a ^{103}In $\rightarrow$ ^{103}Cd calculation is possible in the smaller space of $(\pi p_{1/2},g_{9/2})^{11};(\nu g_{7/2},d_{5/2})^4$ $\rightarrow$ $(\pi p_{1/2},g_{9/2})^{10};(\nu g_{7/2},d_{5/2})^5$, where there are 3527 final states. The N_j factors and total GT strength in the small space are similar to those in the full space, $N_{9/2}$ = 9.0, $N_{7/2}$ = 1.87 and $\sum B_{GT}$ = 12.2. The reason for this is that there is a gap of about 2 MeV between the closely spaced $g_{7/2}$ and $d_{5/2}$ orbitals and the higher $d_{3/2}$, $s_{1/2}$ and $h_{11/2}$ orbitals, and that the wave function is dominated by mixing between the $g_{7/2}$ and $d_{5/2}$ configurations. The B_{GT} distribution obtained in the small space is shown in Fig. 7 in comparison with experiment. The centroid and width of the theoretical distribution is very close to that of the experiment. The main difference in the *shape* of the distributions is that the experiment yields a high-energy tail which is not present in the small-space calculation.

In order to check the importance of the full SNB model space for the details of the GT distribution, we consider the β^+/EC decay ^{101}In $\rightarrow$ ^{101}Cd, where the full-space calculation is possible. The results for the full space, $(\pi p_{1/2}, g_{9/2})^{11}$; $(\nu g_{7/2}, d_{5/2}, d_{3/2}, s_{1/2}, h_{11/2})^2 \rightarrow (\pi p_{1/2}, g_{9/2})^{10}$; $(\nu g_{7/2}, d_{5/2}, d_{3/2}, s_{1/2}, h_{11/2})^3$, and small space, $(\pi p_{1/2}, g_{9/2})^{11}$; $(\nu g_{7/2}, d_{5/2})^2 \rightarrow (\pi p_{1/2}, g_{9/2})^{10}$; $(\nu g_{7/2}, d_{5/2})^3$, are compared in Fig. 8. Again, the total strength is similar in the full SNB and small space. The details of the distributions are different, but the centroids and widths are about the same. One of the differences is that the full-space calculation has more of a high-energy tail (about 10 percent of the

strength lies between 4.5 and 6.0 MeV). Thus we conclude that the tail observed for the ^{103}In experiment is probably related to the configuration mixing in the full model space, that there is very little GT strength predicted above the 6.0 MeV, and that the total strength obtained with the full SNB initial state of ^{103}In should be compared to the total experimental strength (including the high-energy tail) in order to extract a total GT hindrance factor $h_{\rm exp}$.

The total experimental GT strength for ^{103}In, obtained from the average of the two analysis methods is 2.47±0.25, and the total theoretical strength from the SNB calculation is 12.7. Thus, $h_{\rm exp}$ is 5.1±0.5. This is the first time that one has been able to extract this factor close to ^{100}Sn with the confidence that most of the expected strength has been detected experimentally. For the β^+/EC decay of the $N = 50$ isotones discussed in [2], much of the theoretical strength lies at excitation energies above the experimental sensitivity limit. The decay of ^{98}Cd is probably the best case, where only a fraction of about 9% of the total strength is predicted to lie below this limit. For ^{98}Cd, $h_{\rm exp}$ was determined to be $3.8^{+0.7}_{-0.6}$ [2], where the large uncertainty comes partly from the uncertainty in the experimental $Q_{\rm EC}$ value. We note also that this $h_{\rm exp}$ result has an unknown systematical uncertainty as the amount of 9 percent of unobserved GT strength is itself model-dependent.

The $h_{\rm exp}$ values obtained for ^{103}In and ^{98}Cd are marginally consistent with each other. However, it is possible that the higher-order configuration mixing which is responsible for these hindrance factors may have some N and Z dependence. As in [2] one can divide the origin of the hindrance factor into two main classes, namely one (h_a) which involves more nucleons being excited from the $p_{1/2}$,$g_{9/2}$ orbitals to the $g_{7/2}$,$d_{5/2}$,$d_{3/2}$,$s_{1/2}$,$h_{11/2}$ orbitals, and one (h_b) coming from even higher-order mixing with configurations outside the $(p_{1/2},g_{9/2},g_{7/2},d_{5/2},d_{3/2},s_{1/2}, h_{11/2})^n$ model space as well as from the mixing of Δ particles into the nucleon wave functions.

Specifically, h_a is defined as the ratio of the total strength obtained in the SNB model space divided by that obtained in the complete "$0\hbar\omega$" model space $(p_{1/2},g_{9/2},g_{7/2},d_{5/2},d_{3/2},s_{1/2},h_{11/2})^n$. h_b is the ratio of the total strength obtained in the $0\hbar\omega$ model space divided by that obtained in an exact model which includes all possible baryon and meson configurations (mainly nucleon and Δ particle). For practical reasons the total strength is defined as that associated with an excitation energy range expected for the SNB or $0\hbar\omega$ GT final states which extends (for β^+/EC decay in this mass region) up to about 8 MeV excitation energy in the daughter nucleus. By definition, h_a and h_b are multiplicative, and the total hindrance factor h is given by $h = h_a h_b$.

The highest-order effects associated with h_b have been studied in lighter nuclei, where it is possible to explicitly include the $0\hbar\omega$ mixing related to h_a in the wave functions, and then to compare with experiment to obtain h_b. The resulting average value of h_b is 1.68 for the sd shell [18] and 1.81 for the fp shell [19]. As h_b appears to be approximately independent of state and nucleus, it is thus referred to as a global hindrance factor. For the discussion below we will take the average $h_b = 1.75$.

In the sd shell, the calculated value of h_a is nucleus dependent. For example, a comparison [20] of the total $(d_{5/2})^n \rightarrow (d_{5/2})^{n-1}(d_{3/2},s_{1/2})$ β^+ GT strength to the

$(d_{5/2},d_{3/2},s_{1/2})^n \rightarrow (d_{5/2},d_{3/2},s_{1/2})^n$ β^+ GT strength gives $h_a(^{28}\mathrm{Si}) = 2.5$, $h_a(^{26}\mathrm{Mg}) = 3.6$ and $h_a(^{24}\mathrm{Ne}) = 6.2$ ($n = 12$, 10 and 8, respectively). The result for ^{30}Si β^+ decay is $h_a = 3.8$ [21]. Thus one observes an increase in h_a as one goes away from the nominally closed-shell configuration of ^{28}Si. These four cases are structurally analogous to the β^+/EC decay of ^{100}Sn, ^{98}Pd, ^{96}Cd and ^{102}Sn, respectively.

Recently the Monte Carlo shell-model method has been used to calculate h_a values for the $0\hbar\omega$ model space $(g_{9/2},g_{7/2},d_{5/2},d_{3/2}, s_{1/2})^n$. Although the $p_{1/2}$ and $h_{11/2}$ orbitals are not included, they are probably not so important for the value of h_a. The results are (see Table 3 of [22]) $h_a(^{100}\mathrm{Sn}, n = 20) = 1.7$, $h_a(^{98}\mathrm{Cd}, n = 18) = 2.0$, $h_a(^{96}\mathrm{Pd}, n = 16) = 2.5$. (There is a theoretical uncertainty of about 0.1 associated with the Monte Carlo extrapolation method.) Thus again, one observes an increase in h_a as one goes away from the nominally closed-shell configuration of ^{100}Sn. Previous estimates for $h_a(^{100}\mathrm{Sn})$ were 1.25 in a 2p–2h shell-model calculation [2] and an interaction-dependent range of 1.29 to 1.71 obtained in perturbation theory [23]. The exact Monte Carlo results include configurations which go beyond 2p–2h and perturbation theory. (The interpretation of the total GT strength in terms of the N_j occupation numbers given above is only valid for the SNB model space. Once the protons are excited across the $g_{9/2}$-$g_{7/2}$ shell gap, the $\pi g_{7/2} \rightarrow \nu g_{9/2}$ transition is also allowed which destructively interferes with the dominant $\pi g_{9/2} \rightarrow \nu g_{7/2}$ term.)

Thus for ^{98}Cd, taking $h_b = 1.75$ and $h_a = 2.0$, the total hindrance factor is $h(^{98}\mathrm{Cd}) = 3.5$ in good agreement with the experimental value of 3.8 ± 0.7. The Monte Carlo calculation for ^{103}In is not possible. However, one can assume that its hindrance factor should be similar to that of ^{104}Sn. The hindrance factor for ^{104}Sn was not given in [22], but in analogy with the sd-shell results discussed above one could assume $h_a(^{104}\mathrm{Sn}) \approx h_a(^{96}\mathrm{Pd}) = 2.5$. This yields a total calculated hindrance factor of $h = 4.4$ for ^{103}In, which is in reasonable agreement with the experimental value of 5.1 ± 0.4. Thus, we appear to have a nearly quantitative understanding of the hindrance factors for those β^+/EC decays near ^{100}Sn for which the most complete experimental information is available.

5. Summary

We have used the new TAS facility to measure the β-intensity distribution for ^{103}In, a five-quasiparticle configuration with respect to the core nucleus ^{100}Sn. Our experiment confirms the known Q_{EC} value of 6.05(2) MeV, and yields for the first time information on the EC/total ratio (0.445(20)). The resulting values of 3.0–3.2 and 2.5 for the mean γ-ray multiplicity for EC and β^+ decay, respectively, are considerably higher than the result of 2.0 decuced from high-resolution data. The most important results of this work, however, concern the β-intensity distribution:

(i) The total experimental GT strength for ^{103}In was found to be considerably larger (factor 6-7) than that determined in previous high-resolution studies [7], but still reduced by a hindrance factor h_{exp} of 5.1 ± 0.5 compared to the prediction from a full-space shell-model calculation (SNB).

(ii) The experimental B_{GT} distribution for ^{103}In is characterized by a dominant resonance occuring at ^{103}Cd excitation energies of about 3.8 MeV with a full width at half maximum of about 0.7 MeV. Centroid and width of this GT resonance are fairly well reproduced by small-space shell-model calculations. However, the experiment yields a high-energy tail of the B_{GT} distribution, which deviates from the latter calulation. This probably indicates the influence of configuration mixing, as suggested by a comparison of small-space and SNB-space shell-model caluations for ^{101}In.

These results represent an important step in the understanding of the hindrance factors for β^+/EC decays near ^{100}Sn. It is the first time that the *complete* GT strength has been measured so close to ^{100}Sn that a comparison with full-space shell-model calculations becomes possible. Thus, the quality of the data obtained in this work goes beyond that reached in previous experiments for ^{98}Cd [24], ^{100}In [25], ^{103}In [7], ^{100}Sn [26], and ^{100}Ag [8]. In the former four cases, the experimental data are considerably less complete, whereas the latter case is too far away from ^{100}Sn for full-space shell-model calculations.

We emphasize again that it is very important to have the *complete* GT strength from experiment available. This requirement can apparently be fulfilled by the TAS technique. In the future, these experiments will have to be improved along two directions. One the one hand, an improvement of the unfolding procedure is needed in order to reduce the present systematical uncertainties in general and to yield a reliable fine-structure of the GT resonance. On the other hand, the experiments will be pushed closer to ^{100}Sn and eventually to ^{100}Sn itself. It would for example be very interesting to perform TAS measurements for ^{98}Cd, ^{100}In and ^{101}In. A measurement of ^{100}Sn is needed to prove the mass dependence associated with the hindrance factor h_a which relates the SNB model space to the $0\hbar\omega$ model space. In particular, on the basis of the Monte Carlo calculations, one would predict a total hindrance factor of $h = 3.0$ for ^{100}Sn. In addition to the TAS information, one needs improved measurements of Q_{EC} and $T_{1/2}$ in order to extract the GT strength.

The h_a results obtained by Monte Carlo calculations depend on the Hamiltonian in general and on the effective spin–orbit splitting between the $g_{9/2}$ and $g_{7/2}$ orbitals in particular. It will be necessary to calculate this splitting as well as other excited-state properties of the even–even and odd–even nuclei with the next generation of Monte Carlo calculations in order to test and improve upon the Hamiltonian.

Acknowledgements

This work was supported in part by the Polish Committee of Scientific Research under grant KBN 2 P03B 039 13, by C.I.C.Y.T. (Spain) under project AEN96-1662, by the Russian Fund for Basic Research and Deutsche Forschungsgemeinschaft under contract No. 436 RUS 113/201/0(R), by the European Community under contract No. ERBFMGECT950083, and by the U.S. National Science Foundation under grant 9605207. M.K. would like to acknowledge financial support from the Foundation for

Polish Science. B.A.B. wishes to thank the Alexander von Humboldt-Foundation for support. K.R. would like to thank for partial support from the U.S. Department of Energy under DE-AC05-96OR22464 and ORNL managed by Lockheed Martin Energy Research Corporation.

References

[1] E. Roeckl, Nucl. Phys. News 7 (1997) 18.
[2] B.A. Brown and K. Rykaczewski, Phys. Rev. C 50 (1994) R2270.
[3] H. Grawe, M. Górska, M. Lipoglavšek, R. Schubart, A. Atac, A. Axelsson, J. Blomqvist, J. Cederkäll, G. de Angelis, M. de Poli, C. Fahlander, A. Johnson, K.H. Maier, L.-O. Norlin, J. Nyberg, D. Foltescu, M. Palacz, J. Persson, M. Rejmund, H.A. Roth, T. Shizuma, O. Skeppstedt, G. Sletten and M. Weiszflog, Z. Phys. A 358 (1997) 185
[4] I.S. Towner, Nucl. Phys. A 444 (1985) 402
[5] E. Klempt, P. Bob, L. Hornig, J. Last, S.J. Freedman, D. Dubbers and O. Schärpf, Z. Phys. C 37 (1988) 179
[6] S.J. Freedman, Comments Nucl. Part. Phys. 19 (1990) 209
[7] J. Szerypo, R. Grzywacz, Z. Janas, M. Karny, M. Pfützner, A. Płochocki, K. Rykaczewski, J. Żylicz, M. Huyse, G. Reusen, J. Schwarzenberg, P. Van Duppen, A. Wöhr, H. Keller, R. Kirchner, O. Klepper, A. Piechaczek, E. Roeckl, K. Schmidt, L. Batist, A. Bykov, V. Wittmann and B.A. Brown, Z. Phys. A 259 (1997) 117.
[8] L. Batist, A. Bykov, F. Moroz, V. Wittmann, G.D. Alkhazov, H. Keller, R. Kirchner, O. Klepper, E. Roeckl, M. Huyse, P. Van Duppen, G. Reusen, A. Płochocki, M. Pfützner, K. Rykaczewski, J. Szerypo, J. Żylicz and B.A. Brown, Z. Phys. A 351 (1995) 149.
[9] M. Karny, J.M. Nitschke, L.F. Archambault, K. Burkard, D. Cano-Ott, M. Hellström, W. Hüller, R. Kirchner, S. Lewandowski, E. Roeckl and A. Sulik, Nucl. Instr. and Meth. Phys. Res. B 126 (1997) 320.
[10] V.R. Bom, R.W. Hollander, E. Coenen, K. Deneffe, P. Van Duppen and M. Huyse, Z. Phys. A 331 (1988) 21
[11] L. Batist et al., preprint LNPI No. 1547, Gatchina (1989).
[12] K. Burkard, R. Collatz, M. Hellström, Z. Hu, W. Hüller, O. Klepper, R. Kirchner, E. Roeckl, K. Schmidt, M. Shibata and A. Weber, Nucl. Instr. and Meth. Phys. Res. B 126 (1997) 12.
[13] R. Kirchner, Nucl. Instr. and Meth. Phys. Res. B 26 (1987) 204.
[14] D. Cano-Ott, to be published.
[15] W.R. Nelson, H. Hirayama, D.W.O. Rogers, SLAC-report 265 (1985).
[16] B.C. Dzhelepov, L.N. Zyrianova and Yu.P. Suslov, Beta Processes (Nauka, Leningrad, 1972).
[17] N.B. Gove and M.J. Martin, Nucl. Data Tables 10 (1971) 206.
[18] B.A. Brown and B.H. Wildenthal, Ann. Rev. Nucl. Part. Sci. 38 (1988) 29.
[19] G. Martinez-Pinedo, A. Poves, E. Caurier and A.P. Zuker, Phys. Rev. C 53 (1996) R2602.
[20] J. Rapaport, R. Alarcon, B.A. Brown, C. Gaarde, J. Larson, C.D. Goodman, C.C. Foster, D.J. Horen, T. Masterson, E. Sugarbacker and T.N. Taddeucci, Nucl. Phys. A 427 (1984) 332.
[21] B.A. Brown, unpublished.
[22] S.E. Koonin, D.J. Dean and K. Langanke, Phys. Rep. 278 (1997) 1.
[23] I.P. Johnstone, Phys. Rev. C 44 (1991) 1476.
[24] A. Płochocki, K. Rykaczewski, T. Batsch, J. Szerypo, J. Żylicz, R. Barden, O. Klepper, E. Roeckl, D. Schardt, H. Gabelmann, P. Hill, H. Ravn, T. Thorsteinsen, I.S. Grant, H. Grawe, P. Manakos, L.D. Skouras, and the ISOLDE Collaboration, Z. Phys. A 342 (1992) 43.
[25] J. Szerypo, M. Huyse, G. Reusen, P. Van Duppen, Z. Janas, H. Keller, R. Kirchner, O. Klepper, A. Piechaczek, E. Roeckl, D. Schardt, K. Schmidt, R. Grzywacz, M. Pfützner, A. Płochocki, K. Rykaczewski, J. Żylicz, G.D. Alkhazov, L. Batist, A. Bykov, V. Wittmann and B.A. Brown, Nucl. Phys. A 584 (1995) 221.
[26] J. Friese, Proc. Int. Workshop XXIV on Gross Properties of Nuclei and Nuclear Excitations, Hirschegg, Austria (1996), GSI-report, p. 123.